

CRISPR-Cas12a Possesses Unconventional DNase Activity that Can Be Inactivated by Synthetic Oligonucleotides

Bin Li,^{1,2} Jingyue Yan,¹ Youxi Zhang,¹ Wenqing Li,¹ Chunxi Zeng,¹ Weiyu Zhao,¹ Xucheng Hou,¹ Chengxiang Zhang,¹ and Yizhou Dong^{1,3,4,5,6,7}

¹Division of Pharmaceutics and Pharmacology, College of Pharmacy, The Ohio State University, Columbus, OH 43210, USA; ²Department of Infectious Disease, Shenzhen People's Hospital, The Second Clinical Medical College of Jinan University, The First Affiliated Hospital of Southern University of Science and Technology, Shenzhen 518020, China; ³Department of Biomedical Engineering, The Ohio State University, Columbus, OH 43210, USA; ⁴The Center for Clinical and Translational Science, The Ohio State University, Columbus, OH 43210, USA; ⁵James Comprehensive Cancer Center, The Ohio State University, Columbus, OH 43210, USA; ⁶Dorothy M. Davis Heart & Lung Research Institute, The Ohio State University, Columbus, OH 43210, USA; ⁷Department of Radiation Oncology, The Ohio State University, Columbus, OH 43210, USA

CRISPR-Cas12a (CRISPR-Cpf1) was reported to have multiple types of cleavage activities. Without the assistance of CRISPR RNA (crRNA), we investigated DNase activity and substrate specificity of Cas12a orthologs in the presence of diverse divalent metal ions. Cas12a from different species are capable of degrading single-stranded DNA (ssDNA) and/or double-stranded DNA (dsDNA), depending on the metal ions used. In spite of sharing high sequence similarity and functional domains among diverse Cas12a orthologs, only *Acidaminococcus* sp. Cas12a (AsCas12a) showed a predominant preference for cleaving ssDNA, but no detectable activity toward dsDNA substrate in the presence of magnesium (II) ions. In addition, we found that both AsCas12a and *Francisella novicida* Cas12a (FnCas12a) caused substantial dsDNA cleavage in the presence of manganese (II) ion. More importantly, the DNase activities can be inhibited by synthetic DNA oligonucleotides with phosphorothioate linkage modifications. Overall, ssDNase activity of the Cas12a orthologs uncovered a distinct approach for DNA cleavage compared with crRNA-guided dsDNA breaks, and provided insights into potential biological and therapeutic applications.

INTRODUCTION

The class II CRISPR-Cas systems such as CRISPR-Cas9 and CRISPR-Cas12a (also known as CRISPR-Cpf1) utilize a single CRISPR effector module to protect the host against invading genetic elements.^{1–5} Owing to the simplicity and specificity of these systems, they are re-programmed to achieve targeted genome editing, and recently have been applied to clinic trials.^{6,7} Cas12a recognizes double-stranded DNA (dsDNA) by a single CRISPR RNA (crRNA), and thereby induces staggered DNA breaks on the non-targeted and targeted strand via RuvC and Nuc endonuclease domains, respectively.^{5,8–17} Additional functions of Cas12a were also studied in recent years.^{18–23} For example, Cas12a is also demonstrated to be an endoribonuclease that is responsible for processing precursor crRNA into mature

crRNA in a repeat-dependent manner.¹⁸ In the presence of divalent manganese ions (Mn^{2+}), *Francisella novicida* Cas12a (FnCas12a) is able to degrade ssDNA independent of crRNA.¹⁹ In addition, Cas12a is exploited as a quantitative platform for nucleic acids detection because of the unique feature of crRNA-targeted dsDNA-triggered ssDNase cleavage.^{20–23}

In our recent study on synthetic anti-Cas12a oligonucleotides, we found that co-incubation of *Acidaminococcus* sp. Cas12a (AsCas12a) and single-stranded DNA (ssDNA) oligonucleotide in divalent magnesium ions (Mg^{2+})-containing buffer led to the degradation of ssDNA.²⁴ This observation of AsCas12a was different from that of FnCas12a.¹⁹ Upon further investigation of the substrate specificity of two additional Cas12a orthologs, *Lachnospiraceae* bacterium Cas12a (LbCas12a) and FnCas12a,^{5,25–27} herein we report that different divalent metal ions are required for different Cas12a orthologs to induce DNase activities. Like FnCas12a, the crRNA-independent DNase activity of LbCas12a can be activated only by Mn^{2+} , whereas AsCas12a is able to degrade DNA substrates in the presence of Mg^{2+} and/or Mn^{2+} . Furthermore, Mn^{2+} is able to trigger both AsCas12a- and FnCas12a-mediated dsDNA cleavage, which is not observed for LbCas12a. Of note, these Cas12a-mediated DNA cleavage activities can be inhibited by synthetic anti-Cas12a oligonucleotides. Taken together, these findings expand our understanding of the cleavage patterns of Cas12a orthologs and demonstrate that the crRNA-independent DNase activities of the Cas12a orthologs can be regulated by synthetic oligonucleotides.

Received 5 September 2019; accepted 27 December 2019;
<https://doi.org/10.1016/j.omtn.2019.12.038>

Correspondence: Yizhou Dong, Division of Pharmaceutics and Pharmacology, College of Pharmacy, The Ohio State University, Columbus, OH 43210, USA.
E-mail: dong.525@osu.edu



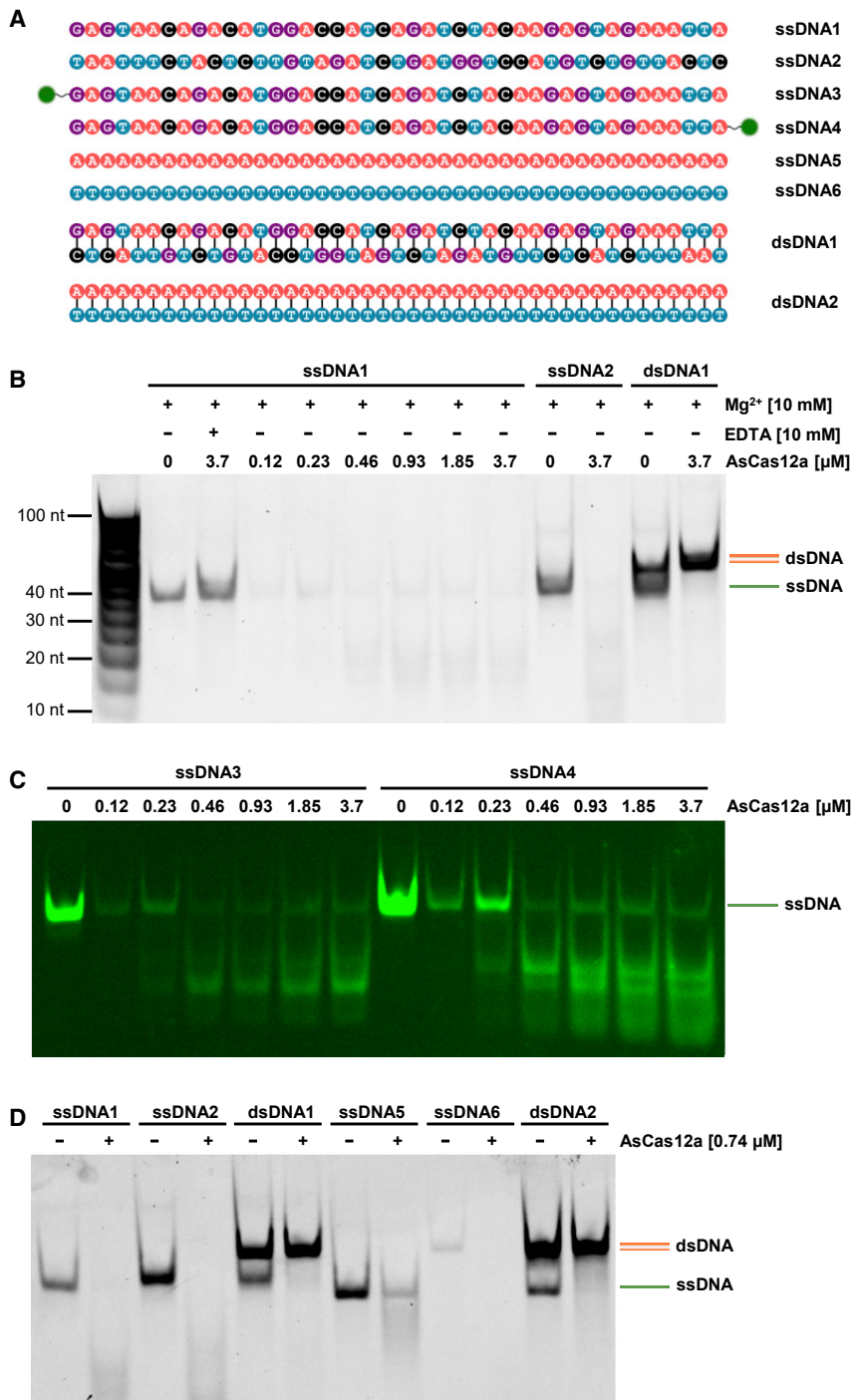


Figure 1. crRNA-Free DNase Activities of Cas12a Orthologs toward Linear DNA Oligonucleotides

(A) Graphical illustration of DNA oligonucleotide substrates used in this study. The filled green circle indicates fluorescent probe Cy3. (B) Dose-response and substrate specificity of AsCas12a toward single-stranded DNA (ssDNA) and double-stranded DNA (dsDNA) oligonucleotides. (C) Cleavage activity of AsCas12a on fluorescently labeled ssDNA oligonucleotide. (D) Effects of hairpin structure on DNase activity of AsCas12a. DNA oligonucleotides with or without hairpin structure can be degraded by AsCas12a.

blocked AsCas12a-mediated genome-editing activity, whereas unmodified ssDNA counterparts (ssDNA1; Figure 1A) were subjected to cleavage by AsCas12a in the Mg²⁺-containing reaction buffer without crRNA.²⁴ As shown in Figure 1B, ssDNA1 and its complementary strand (ssDNA2; Figure 1A) were cleaved into small fragments when they were exposed to a wide range of concentrations of AsCas12a, whereas the annealed 43-bp dsDNA (dsDNA1; Figure 1A) was not degraded even at the highest concentration of AsCas12a tested. Like other metalloenzymes, AsCas12a required Mg²⁺ as a cofactor to exert its enzymatic activity, and the Mg²⁺-dependent ssDNase activity can be inactivated by EDTA metal chelator (Figure 1B). These results demonstrated that AsCas12a was able to cleave ssDNA in the presence of Mg²⁺, and suggested that different mechanisms may exist between crRNA-independent ssDNase activity and previously reported crRNA/target DNA activation-triggered ssDNA cleavage.^{20,21,23} To determine whether the observed degradation was caused by endonucleolytic or exonucleolytic processing of substrates, we examined DNase activity of AsCas12a further on both 5' and 3' end-labeled ssDNAs (ssDNA3 and ssDNA4; Figure 1A). As shown in Figure 1C, the cleaved fragments produced by AsCas12a were heterogeneous in size rather than progressive shortening of the labeled substrate no matter which end of ssDNA1 was fluorescently labeled, indicating that AsCas12a possesses endonuclease activity.

We next performed a BLAST search against the UniProt Knowledgebase using AsCas12a (UniProt: U2UMQ6) as a query sequence,^{5,28} and identified three SbcC proteins that share sequence similarity with AsCas12a (Figure S1). Also, the sequence comparison was conducted for LbCas12a and FnCas12a (Figure S1). Among the six proteins aligned, FnCas12a displayed an extremely high degree of sequence similarity (99.0%) to SbcC protein from *Francisella tularensis* subsp. *novicida* PA10-7858

RESULTS

DNase Activities of Cas12a Orthologs on Linear DNA in the Absence of crRNA

During our previous study of anti-Cas12a oligonucleotides, we observed that phosphorothioate (PS)-modified DNA oligonucleotides (termed anti-Cas12a psDNA; Table S1) with the same length of crRNA (43 nt)

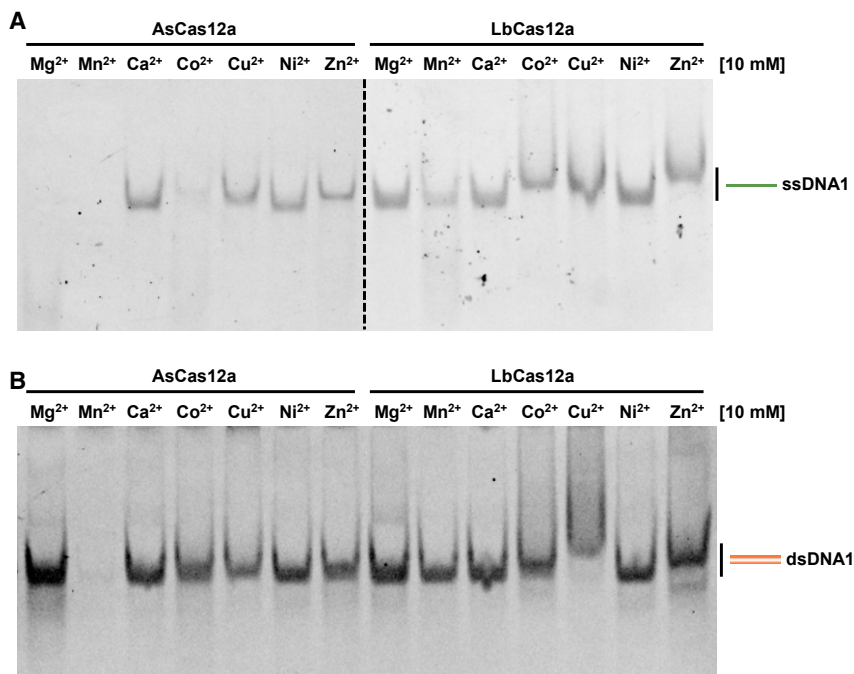


Figure 2. Metal Ion Effects on Cas12a Activity toward Linear DNA Oligonucleotides

(A and B) Representative *in vitro* cleavage of ssDNA1 (A) and dsDNA1 (B) oligonucleotides by AsCas12a and LbCas12a in the presence of various divalent metal ions, including Mg²⁺, Mn²⁺, Ca²⁺, Co²⁺, Cu²⁺, Ni²⁺, and Zn²⁺. The vertical dotted line indicates the border between two separate gels. Positions of ssDNA1 and dsDNA1 were indicated.

(FnSbcC, UniProt: A0A1I9YB83) (Figure S1), a type of rare bacteria isolated from human clinical specimens.²⁹ Considering the sequence similarity with the SbcC family, an enzyme acting on hairpin structure,^{30–33} we also examined cleavage activity of AsCas12a on the 43-nt polyA or polyT ssDNA substrates without hairpin structures (ssDNA5 and ssDNA6; Figure 1A) at a molar ratio of 10:1 (AsCas12a:polynucleotides). Like ssDNA1 and ssDNA2, both polyA and polyT ssDNA were degraded by AsCas12a, implicating that AsCas12a did not require hairpin structures to exert endonuclease activity (Figure 1D). Meanwhile, 43-bp dsDNA (dsDNA2) formed by annealing of polyA and polyT was tolerated to AsCas12a-mediated cleavage (Figure 1D). These results were in agreement with the above conclusion that AsCas12a in the Mg²⁺ buffer displayed a preferred endonuclease activity to ssDNA other than dsDNA.

Effects of Divalent Metal Ions on DNase Activity of Cas12a Orthologs

To investigate the effects of divalent metal ions on DNase activities of Cas12a orthologs, we tested a panel of divalent ions in the cleavage reactions. As shown in Figure 2A, AsCas12a led to complete degradation of ssDNA1 in the presence of Mg²⁺ and Mn²⁺, and induced almost full cleavage in the buffer containing Co²⁺. In the case of LbCas12a, more than 50% of crRNA-independent DNase activity was detected in the Mn²⁺ buffer. All other divalent metal ions, including Ca²⁺, Cu²⁺, Ni²⁺, and Zn²⁺, were not served as effective cofactors for Cas12a orthologs tested. Next, we evaluated both AsCas12a and LbCas12a behaviors on dsDNA1 with these ions. Notably, AsCas12a led to significant cleavage of dsDNA in the presence of Mn²⁺. By contrast, none of the divalent metal ions

triggered LbCas12a-mediated dsDNase activity (Figure 2B). Different divalent ion requirements for DNase activity among AsCas12a and LbCas12a, as well as previously reported FnCas12a, revealed that diverse Cas12a orthologs possess different preference to metal ions.

The Cleavage Pattern of Cas12a Orthologs on Covalently Closed Circular DNA

We next extended the substrate to covalently closed circular DNA. AsCas12a was able to degrade M13mp18 circular ssDNA in a dose-dependent manner (Figure S2), indicating that

free 5' phosphate and 3' hydroxyl DNA ends are not essential for the enzymatic activity. The endonucleolytic activity of AsCas12a on circular ssDNA was in accordance to the results obtained from Figure 1C. To determine the metal ion dependency of circular DNA cleavage by Cas12a, we performed enzyme assays with various divalent metal ions as mentioned above. Similarly, the enzymatic activity of Cas12a orthologs on covalently closed circular DNA was dependent upon the presence of a divalent ion (Figure 3A). AsCas12a displayed robust cleavage activity on M13mp18 in both Mg²⁺ and Mn²⁺ buffers, and induced approximately 50% degradation of M13mp18 ssDNA in the Co²⁺ buffer (Figure 3A). On the other hand, LbCas12a was active with Mn²⁺, but not with Mg²⁺, in a manner similar to FnCas12a (Figure 3A). No significant cleavage activity was observed for Cas12a in other metal ions tested (Figure 3A). To investigate the effects of divalent and trivalent iron ions and the counterion on the DNase activity of the CRISPR-Cas12a system, we also performed *in vitro* cleavage assays in the solutions of FeCl₂, FeCl₃, Mg(NO₃)₂, and Mn(NO₃)₂. As shown in Figure S3, Fe²⁺ and Fe³⁺ ions were able to trigger RNA-independent DNase activities and resulted in complete substrate cleavage. Cas12a remained active when MgCl₂ or MnCl₂ was replaced with Mg(NO₃)₂ or Mn(NO₃)₂ (Figure S3).

Although AsCas12a cleaved M13mp18 circular ssDNA equally well in 10 mM Mg²⁺ and Mn²⁺, the cleavage efficiency with Mn²⁺ for AsCas12a was significantly higher than that in the Mg²⁺ buffer when low concentrations of metal ions were present (Figure 3B). For instance, AsCas12a completely degraded M13mp18 in 0.2 and 0.5 mM Mn²⁺, whereas no detectable activity was observed

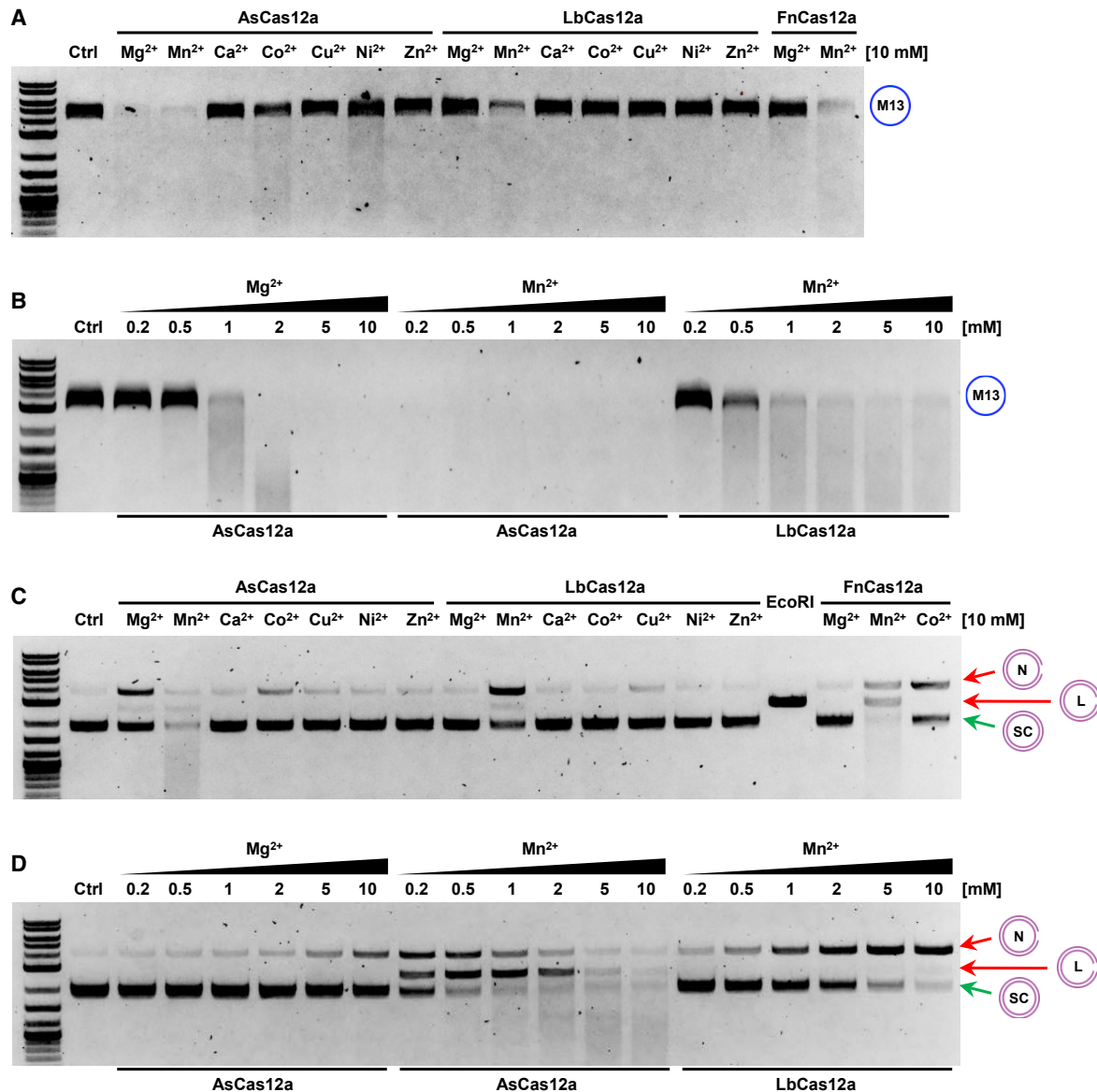


Figure 3. crRNA-Free DNase Activities of Cas12a Orthologs toward Circular DNA

(A) Representative *in vitro* cleavage of circular phage M13mp18 ssDNA by AsCas12a and LbCas12a in the presence of various divalent metal ions. FnCas12a was used as a positive group. Control (Ctrl), M13mp18 ssDNA alone. (B) Metal ion concentration dependence for cleavage of M13mp18 ssDNA substrates by AsCas12a and LbCas12a. Different concentrations of Mg²⁺ or Mn²⁺ ranging from 0.5 to 10 mM were used. Ctrl, M13mp18 ssDNA alone. (C) Representative *in vitro* cleavage of circular plasmid pUC19 dsDNA by AsCas12a and LbCas12a in the presence of various divalent metal ions. FnCas12a was used as a positive group. Ctrl, pUC19 dsDNA alone. (D) Metal ion concentration dependence for cleavage of pUC19 dsDNA substrates by AsCas12a and LbCas12a. Different concentrations of Mg²⁺ or Mn²⁺ ranging from 0.5 to 10 mM were used. Ctrl, pUC19 dsDNA alone. Positions of M13mp18, supercoiled (SC, green arrow), nicked (N, red arrow), and linear (L, red arrow) DNA were indicated.

under the same condition of Mg²⁺ (Figure 3B). With an increase of the Mn²⁺ concentrations from 0.2 to 10 mM, more than 95% of the M13mp18 substrate was subjected to degradation but was not completely digested by LbCas12a (Figure 3B). In addition to M13mp18 ssDNA, the metal-dependent degradation activities of Cas12a orthologs were also validated when bacteriophage ΦX174 (Figure 6C) was used as the circular ssDNA substrate.

To study the substrate specificity of Cas12a orthologs, we then investigated covalently closed circular dsDNA pUC19. Likewise, AsCas12a was active in the presence of Mg²⁺ and Mn²⁺, and LbCas12a functioned well in Mn²⁺. It was noteworthy that incubation of AsCas12a with pUC19 in Mg²⁺ caused a similar cleavage behavior as LbCas12a did in Mn²⁺, where the supercoiled pUC19 was converted into nicked, but not linear, form (Figure 3C). In contrast, the enzyme action of

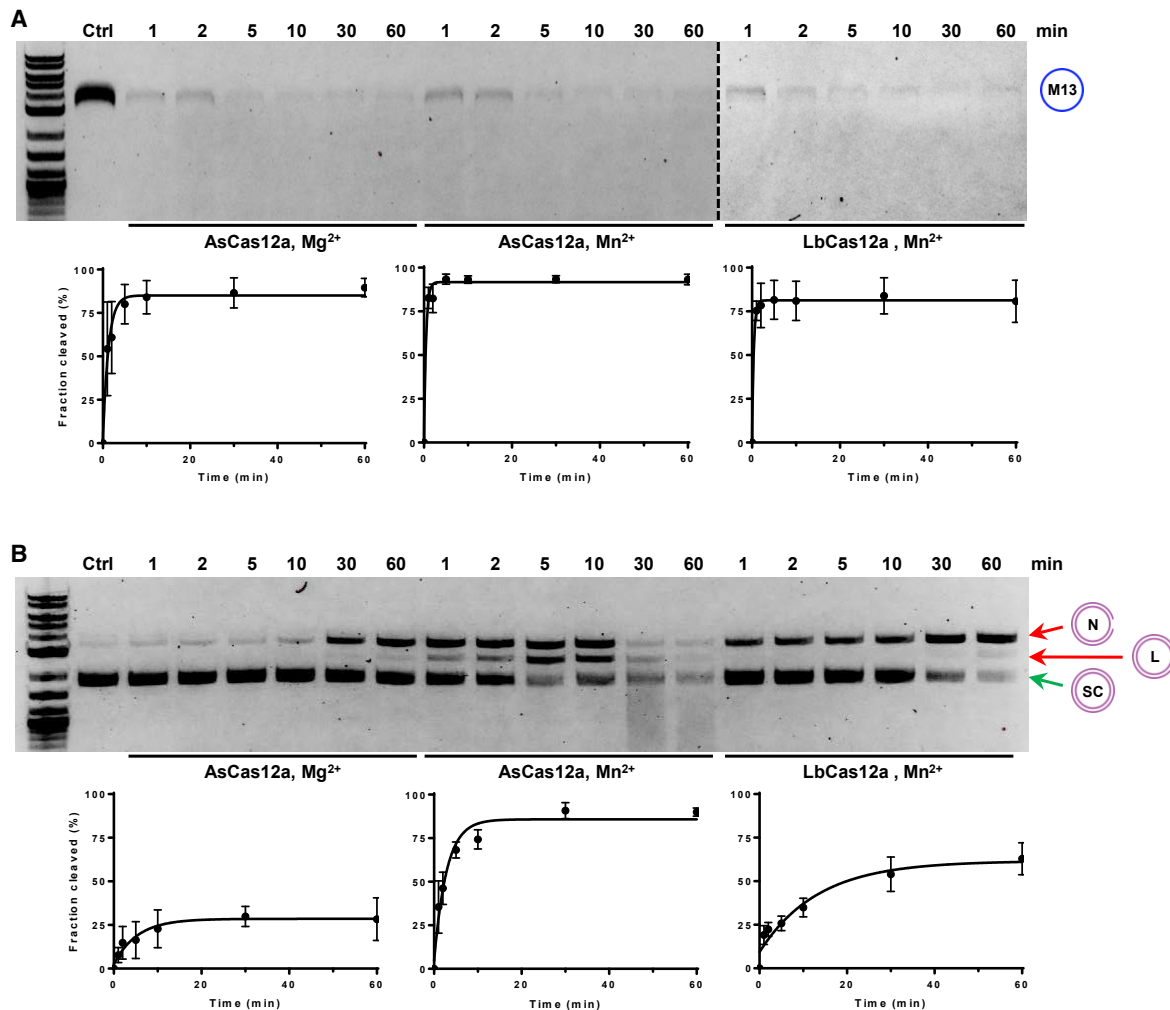


Figure 4. Time Course of Degradation of DNA Substrates by Cas12a

(A and B) Representative gel images of Cas12a activity toward M13mp18 ssDNA (A) and pUC19 dsDNA (B) at indicated time points (min) were shown in the upper panel. Positions of M13, supercoiled (SC), nicked (N), and linear (L) DNA were indicated. The vertical dotted line indicates the border between two separate gels. The fraction cleaved (%) from three independent experiments is plotted against the time points (min) and fitted with a nonlinear regression in the lower panel. Error bars are presented as mean \pm SEM.

AsCas12a in Mn²⁺ and FnCas12a in Mn²⁺ was different from those observations (Figure 3C). In this case, pUC19 was first nicked on one strand and then further cleaved on the other strand to form linear DNA. Finally, the nicked and linear pUC19 were degraded into smaller fragments, as evidenced by the smear bands below the cleaved products with high band intensity (Figure 3C). Substitution of Mg²⁺ and Mn²⁺ with the remaining divalent metals ions, such as Ca²⁺, Cu²⁺, Ni²⁺, and Zn²⁺, led to minimal cleavage fragments produced by Cas12a (Figure 3C). Lastly, we linearized circular pUC19 dsDNA with the EcoRI restriction enzyme to mimic genomic DNA. In accordance with the findings in Figure 2B, only AsCas12a showed robust dsDNase activity (70%) in buffers containing Mn²⁺ (Figure S4). Moreover, we noticed that the control group FnCas12a also exhibited comparable cleavage activity to AsCas12a on the

long linearized pUC19 dsDNA substrate in the presence of Mn²⁺ (Figure S4), which was consistent with the results obtained from circular dsDNA pUC19 (Figure 3C). Also, FnCas12a resulted in substantial short dsDNA oligonucleotide degradation in the presence of Mn²⁺ (Figure 5B, lane 5). These experimental data are not the same as the previous results that FnCas12a does not result in cleavage of linear dsDNA.¹⁹

To investigate the effects of metal ions concentration on endonuclease activity, we examined cleavage activity with varying concentrations of Mg²⁺ or Mn²⁺. As shown in Figure 3D, when the concentration of Mg²⁺ is increased from 0.2 to 10 mM, only a small fraction of supercoiled pUC19 (<25%) was converted to nicked form by AsCas12a. However, the majority of pUC19 substrate disappeared

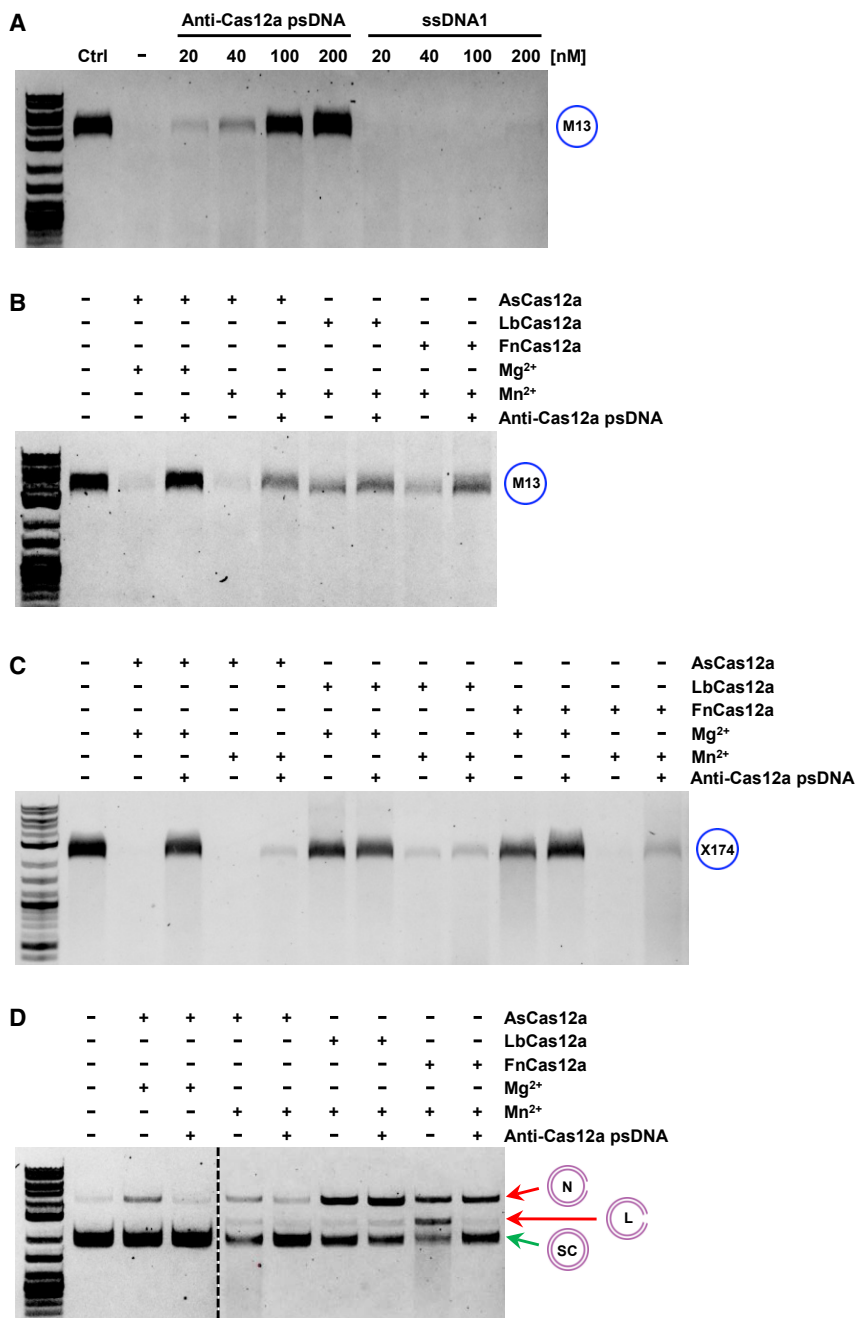


Figure 6. Inhibitory Effects of Anti-Cas12a psDNA on Cas12a-Mediated DNase Activity toward Circular DNA

(A) Dose-dependent inhibitory effects of anti-Cas12a psDNA on Mg²⁺-promoted AsCas12a activity. Control (Ctrl), M13mp18 ssDNA alone. ssDNA1 was parallelly used to rule out the possibility of oligonucleotides interference. The concentration of AsCas12a was 200 nM. (B–D) The effects of anti-Cas12a psDNA on metal-dependent ssDNase activity of Cas12a orthologs (AsCas12a, LbCas12a, and FnCas12a) on circular ssDNA M13mp18 (B), ΦX174 (C), and dsDNA pUC19 (D). The concentration of anti-Cas12a psDNA was 200 nM. Ctrl, M13mp18 ssDNA alone. The vertical dotted line indicates the border between two separate gels. Ctrl, pUC19 dsDNA alone. Positions of M13, ΦX174, supercoiled (SC), nicked (N), and linear (L) DNA were indicated.

(Figure 6A). Mg²⁺-promoted AsCas12a activity was completely inhibited in the presence of 200 mM anti-Cas12a psDNA (Figures 6A and 6B). Under the same situations, however, the presence of anti-Cas12a psDNA resulted in only partial loss of the nuclease activity of AsCas12a in Mn²⁺ and FnCas12a in Mn²⁺ (Figure 6B). The introduction of anti-Cas12a psDNA did not affect much LbCas12a function in Mn²⁺ (Figure 6B). Meanwhile, anti-Cas12a psDNA exhibited a similar Cas12a inhibitory profile to ΦX174 ssDNA (Figure 6C). Similar inhibitory effects occurred when circular dsDNA substrates were used (Figure 6D). It is notable that, for circular dsDNA, the anti-Cas12a psDNA inhibitor lacked the capacity to block the nicking activity of FnCas12a, but remarkably inhibited the formation of linearized products in the presence of Mn²⁺ (Figure 6D). Overall, these findings suggested that anti-Cas12a oligonucleotides are effective inhibitors for Cas12a's DNase activity.

Based on the above results, we found that Cas12a orthologs displayed distinct crRNA-independent DNase activities toward different DNA substrates, depending on the divalent

metal ions presented (Figures 7A and 7B). The substrate specificity of Cas12a might be exploited by bacteria to protect themselves from ssDNA viral invasion. Moreover, we showed that synthetic anti-Cas12a oligonucleotides that contain PS linkages inhibited Cas12a-mediated DNase activity, with the strongest inhibitory effects for AsCas12a (Figure 7C). Taken together, these results demonstrated that both ssDNase and dsDNase activity of Cas12a can be triggered by divalent metal ions and were tunable using anti-Cas12a oligonucleotides.

dsDNA3 (annealed pair of ssDNA2 and ssDNA3) and linearized pUC19 in the presence of Mn²⁺ (Figures 5B and 5C).

Next, we investigated the inhibition on circular DNA substrates (Figure 6). Although the addition of ssDNA1 (the counterpart of anti-Cas12a psDNA) did not affect ssDNase activity even at a concentration of 200 mM, the extent of inhibition of circular M13mp18 ssDNA degradation by AsCas12a in Mg²⁺ was dramatically increased with the increased amount of anti-Cas12a psDNA

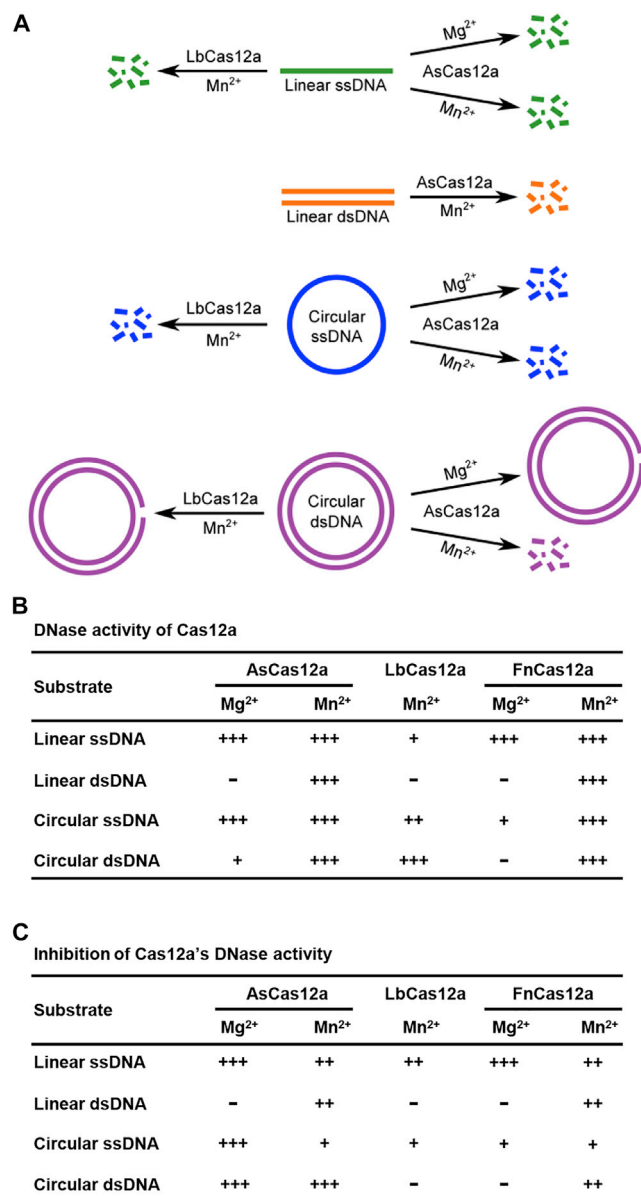


Figure 7. Summary of DNase Activity of Cas12a Orthologs, as well as Inhibitory Activity of Anti-Cas12a psDNA Inhibitor

(A) Schematic of DNase activity of Cas12a orthologs on various substrates tested, including linear ssDNA, linear dsDNA, circular ssDNA, and circular dsDNA. (B) Summary of DNase activity of Cas12a orthologs toward different DNA substrates. (C) Summary of inhibition activity of anti-Cas12a psDNA against Cas12a orthologs. -, no significant activity; +, weak activity; ++, medium activity; +++, full activity.

DISCUSSION

In this study, we demonstrate that Cas12a orthologs are capable of cleaving multiple types of DNA in the absence of crRNA. The ssDNase and dsDNase activities of Cas12a orthologs require activation by different divalent metal ions depending on the Cas12a orthologs. Despite sharing the high sequence similarity and conserved cat-

alytic domains (RuvC and Nuc endonuclease domains) among Cas12a orthologs,⁵ AsCas12a, LbCas12a, and FnCas12a show distinct physicochemical characteristics in metal ion dependence, substrate specificity, cleavage efficiency and rate, and sensitivity to synthetic Cas12a inhibitor. Whereas LbCas12a and FnCas12a are active only in the presence of Mn²⁺, both Mg²⁺ and Mn²⁺ trigger AsCas12a-mediated ssDNase activity. In addition, Mg²⁺-promoted ssDNA cleavage by AsCas12a was not observed for dsDNA substrates. Given the different cleavage behavior of Cas12a on ssDNA and dsDNA substrates in different metal ions (Figure 7), we speculated that bacteria might utilize their CRISPR-Cas12a system to prevent ssDNA viral infections. In addition, we also found that both AsCas12a and FnCas12a displayed robust crRNA-independent cleavage activity on linear dsDNA substrates in the presence of Mn²⁺, highlighting the importance of using Mn²⁺ with caution to minimize unintended genomic DNA breaks induced by Cas12a. These results suggest that there are substantial mechanistic differences between RNA-guided endonuclease activity and RNA-independent DNase activity. More importantly, the crRNA-independent cleavage behaviors of Cas12a orthologs can be controlled by chemically modified DNA oligonucleotides, which is an effective approach to regulate DNase activities of Cas12a orthologs. The diversity of crRNA-independent cleavage approaches by Cas12a reported here reflects potential evolution diversity of these adaptive CRISPR-Cas12a systems and provides insights into understanding the origin and evolution of the CRISPR-Cas12a system.

MATERIALS AND METHODS

Cas12a Protein and DNA Substrates

AsCas12a protein is a gift from New England Biolabs. LbCas12a protein, circular single-stranded phage DNA M13mp18 (7,249 bases in length), Φ X174 (5,386 bases in length), and circular double-stranded plasmid DNA pUC19 (2,686 bp in length) are obtained from New England Biolabs. FnCas12a protein is from Applied Biological Materials. All oligonucleotides (Table S1) were synthesized by Integrated DNA Technologies or Eurofins Genomics. The ssDNA oligonucleotide ssDNA1 has a complementary sequence to crRNA targeting *DNMT1* locus. ssDNA2 is complementary to ssDNA1. Cy3-labeled ssDNA1 at the 5' (ssDNA3) or 3' end (ssDNA4) was used to determine the endonuclease activity. Oligonucleotides A₄₃ (ssDNA5) and T₄₃ (ssDNA6) were used to assess the hairpin-dependent activity.

Generation of Linear dsDNA

The dsDNA oligonucleotide dsDNA1 was generated through annealing ssDNA1 with equimolar amounts of complementary ssDNA2 in a total volume of 20 μ L of nuclease-free water with the following program: initial denaturation at 95°C for 30 s and then cooldown from 95°C to 25°C with 1°C decrease per minute using a thermocycler T-100 (Bio-Rad). The dsDNA oligonucleotides dsDNA2 and dsDNA3 were prepared by annealing two complementary oligonucleotides, ssDNA5 and ssDNA6, and ssDNA2 and ssDNA3, with the same procedures. Linearized pUC19 was obtained by digesting 4 μ g of pUC19 dsDNA with 2 μ L (20 U/ μ L) of EcoRI-HF

(New England Biolabs) in a total reaction volume of 200 μL of reaction buffer (50 mM potassium acetate, 20 mM Tris-acetate, 10 mM magnesium acetate, 100 $\mu\text{g}/\text{mL}$ BSA) for 1 h at 37°C. Linearized pUC19 was purified with a QIAquick PCR purification kit (QIAGEN) according to the manufacturer's instructions and stored at -80°C prior to use.

In Vitro Cleavage Assay

Unless otherwise stated, standard *in vitro* cleavage reactions were conducted in a total volume of 5 μL of cleavage buffer containing 50 mM NaCl, 10 mM Tris-HCl (pH 7.9), and 1 mM DTT, supplemented with 10 mM divalent metal ions or 10 mM EDTA, and quenched by Proteinase K. For the dose-dependent assay, linear ssDNA1 substrate (74 nM) was incubated with increasing concentrations of AsCas12a protein (from 120 to 3,700 nM) in the presence of 10 mM Mg^{2+} at 37°C for 30 min; in the case of circular substrate, circular M13mp18 ssDNA (2 nM) was incubated with AsCas12a protein (from 20 to 200 nM) in 10 μL of cleavage buffer containing 10 mM Mg^{2+} at 37°C for 30 min. DNase activities toward linear DNA oligonucleotides (74 nM) were measured at a fixed molar ratio of 1:100 (linear DNA:Cas12a protein). For circular M13mp18 (2 nM), ΦX174 (6 nM), pUC19 (4 nM), and linearized pUC19 (4 nM), the molar ratio was fixed at 1:100 (circular DNA:Cas12a protein). Cleaved fractions were separated on a native 15% polyacrylamide Tris-borate-EDTA (TBE) gel for both linear ssDNA and linear dsDNA oligonucleotides, and 1% agarose gel for circular M13mp18 and ΦX174 ssDNA, circular pUC19 dsDNA, and linearized pUC19 dsDNA. The polyacrylamide TBE gel and agarose gel were respectively stained with SYBR Gold and EZ-Vision In-Gel staining, visualized using the ChemiDoc MP Imaging System (Bio-Rad), and analyzed by the Image Lab analysis software (Bio-Rad Laboratories).

Measurements of Metal Ion Activation of Enzyme Reaction

Inorganic salts including MgCl_2 , MnCl_2 , CaCl_2 , CoCl_2 , CuCl_2 , NiCl_2 , ZnCl_2 , FeCl_2 , FeCl_3 , and $\text{Mg}(\text{NO}_3)_2$ were from Thermo Fisher Scientific with a minimum purity of 99.99%. $\text{Mn}(\text{NO}_3)_2$ with 98% purity was from Sigma-Aldrich. Stock solutions (100 mM) were prepared by dissolving inorganic salts in nuclease-free water. Unless otherwise stated, metal-dependent nuclease activity was measured in the presence of 10 mM divalent metal ion or 10 mM EDTA. For metal ion concentration-dependent assay, increasing concentrations of metal ions (from 0.2 to 10 mM) were incubated with either 2 nM circular M13mp18 ssDNA or 4 nM circular pUC19 dsDNA in the presence of Mg^{2+} or Mn^{2+} for 30 min at 37°C. Reactions were terminated by adding 1 μL of Proteinase K. For kinetic study, reactions were quenched at different time points and were run on 1% agarose gel. Error bars are presented as mean \pm SEM.

Inhibition of Cas12a-Mediated DNase Activity by Anti-Cas12a psDNA

Anti-Cas12a psDNA bearing PS linkage modifications was synthesized by Integrated DNA Technologies. To study dose-dependent inhibition effects, we incubated increasing concentrations of anti-Cas12a psDNA (from 20 to 200 nM) with M13mp18 (2 nM) and

AsCas12a (200 nM) in the presence of 10 mM Mg^{2+} at 37°C for 30 min. Inhibition of crRNA-independent DNase activities of Cas12a orthologs toward ssDNA (2 nM M13mp18, 6 nM ΦX174 , or 74 nM ssDNA3) and dsDNA (4 nM circular or linearized pUC19, or 74 nM dsDNA3) was carried out by adding equimolar anti-Cas12a psDNA over Cas12a protein to the standard reaction.

SUPPLEMENTAL INFORMATION

Supplemental Information can be found online at <https://doi.org/10.1016/j.omtn.2019.12.038>.

AUTHOR CONTRIBUTIONS

B.L. and Y.D. conceived and designed the experiments. B.L., J.Y., and Y.Z. conducted the experiments. B.L., J.Y., Y.Z., W.L., C.Z., W.Z., X.H., C.Z., and Y.D. analyzed the data. B.L. and Y.D. wrote the paper. The final manuscript was edited and approved by all authors.

CONFLICTS OF INTEREST

The authors declare no competing interests.

ACKNOWLEDGMENTS

We thank New England Biolabs for generously providing AsCas12 protein. This work was supported by the NIH through the National Heart, Lung, and Blood Institute (grant R01HL136652), as well as by the start-up fund from the College of Pharmacy at The Ohio State University.

REFERENCES

- Jinek, M., Chylinski, K., Fonfara, I., Hauer, M., Doudna, J.A., and Charpentier, E. (2012). A programmable dual-RNA-guided DNA endonuclease in adaptive bacterial immunity. *Science* 337, 816–821.
- Gasiunas, G., Barrangou, R., Horvath, P., and Siksnys, V. (2012). Cas9-crRNA ribonucleoprotein complex mediates specific DNA cleavage for adaptive immunity in bacteria. *Proc. Natl. Acad. Sci. USA* 109, E2579–E2586.
- Cong, L., Ran, F.A., Cox, D., Lin, S., Barretto, R., Habib, N., Hsu, P.D., Wu, X., Jiang, W., Marraffini, L.A., and Zhang, F. (2013). Multiplex genome engineering using CRISPR/Cas systems. *Science* 339, 819–823.
- Mali, P., Yang, L., Esvelt, K.M., Aach, J., Guell, M., DiCarlo, J.E., Norville, J.E., and Church, G.M. (2013). RNA-guided human genome engineering via Cas9. *Science* 339, 823–826.
- Zetsche, B., Gootenberg, J.S., Abudayyeh, O.O., Slaymaker, I.M., Makarova, K.S., Essletzbichler, P., Volz, S.E., Joung, J., van der Oost, J., Regev, A., et al. (2015). Cpf1 is a single RNA-guided endonuclease of a class 2 CRISPR-Cas system. *Cell* 163, 759–771.
- Mullard, A. (2018). Industry advances landmark CRISPR candidate into the clinic. *Nat. Rev. Drug Discov.* 17, 697.
- Li, B., Niu, Y., Ji, W., and Dong, Y. (2020). Strategies for the CRISPR-Based Therapeutics. *Trends Pharmacol. Sci.* 41, 55–65.
- Yamano, T., Nishimasu, H., Zetsche, B., Hirano, H., Slaymaker, I.M., Li, Y., Fedorova, I., Nakane, T., Makarova, K.S., Koonin, E.V., et al. (2016). Crystal Structure of Cpf1 in Complex with Guide RNA and Target DNA. *Cell* 165, 949–962.
- Dong, D., Ren, K., Qiu, X., Zheng, J., Guo, M., Guan, X., Liu, H., Li, N., Zhang, B., Yang, D., et al. (2016). The crystal structure of Cpf1 in complex with CRISPR RNA. *Nature* 532, 522–526.
- Stella, S., Alc3n, P., and Montoya, G. (2017). Structure of the Cpf1 endonuclease R-loop complex after target DNA cleavage. *Nature* 546, 559–563.

11. Gao, P., Yang, H., Rajashankar, K.R., Huang, Z., and Patel, D.J. (2016). Type V CRISPR-Cas Cpf1 endonuclease employs a unique mechanism for crRNA-mediated target DNA recognition. *Cell Res.* 26, 901–913.
12. Swarts, D.C., van der Oost, J., and Jinek, M. (2017). Structural Basis for Guide RNA Processing and Seed-Dependent DNA Targeting by CRISPR-Cas12a. *Mol. Cell* 66, 221–233.e4.
13. Strohkendl, I., Saifuddin, F.A., Rybarski, J.R., Finkelstein, I.J., and Russell, R. (2018). Kinetic Basis for DNA Target Specificity of CRISPR-Cas12a. *Mol. Cell* 71, 816–824.e3.
14. Singh, D., Mallon, J., Poddar, A., Wang, Y., Tippana, R., Yang, O., Bailey, S., and Ha, T. (2018). Real-time observation of DNA target interrogation and product release by the RNA-guided endonuclease CRISPR Cpf1 (Cas12a). *Proc. Natl. Acad. Sci. USA* 115, 5444–5449.
15. Jeon, Y., Choi, Y.H., Jang, Y., Yu, J., Goo, J., Lee, G., Jeong, Y.K., Lee, S.H., Kim, I.-S., Kim, J.-S., et al. (2018). Direct observation of DNA target searching and cleavage by CRISPR-Cas12a. *Nat. Commun.* 9, 2777.
16. Li, B., Zhao, W., Luo, X., Zhang, X., Li, C., Zeng, C., and Dong, Y. (2017). Engineering CRISPR-Cpf1 crRNAs and mRNAs to maximize genome editing efficiency. *Nat. Biomed. Eng.* 1, 0066.
17. Li, B., Zeng, C., and Dong, Y. (2018). Design and assessment of engineered CRISPR-Cpf1 and its use for genome editing. *Nat. Protoc.* 13, 899–914.
18. Fonfara, I., Richter, H., Bratovič, M., Le Rhun, A., and Charpentier, E. (2016). The CRISPR-associated DNA-cleaving enzyme Cpf1 also processes precursor CRISPR RNA. *Nature* 532, 517–521.
19. Sundaresan, R., Parameshwaran, H.P., Yogesha, S.D., Keilbarth, M.W., and Rajan, R. (2017). RNA-Independent DNA Cleavage Activities of Cas9 and Cas12a. *Cell Rep.* 21, 3728–3739.
20. Chen, J.S., Ma, E., Harrington, L.B., Da Costa, M., Tian, X., Palefsky, J.M., and Doudna, J.A. (2018). CRISPR-Cas12a target binding unleashes indiscriminate single-stranded DNase activity. *Science* 360, 436–439.
21. Stella, S., Mesa, P., Thomsen, J., Paul, B., Alcón, P., Jensen, S.B., Saligram, B., Moses, M.E., Hatzakis, N.S., and Montoya, G. (2018). Conformational Activation Promotes CRISPR-Cas12a Catalysis and Resetting of the Endonuclease Activity. *Cell* 175, 1856–1871.e1821.
22. Li, S.-Y., Cheng, Q.-X., Wang, J.-M., Li, X.-Y., Zhang, Z.-L., Gao, S., Cao, R.-B., Zhao, G.-P., and Wang, J. (2018). CRISPR-Cas12a-assisted nucleic acid detection. *Cell Discov.* 4, 20.
23. Gootenberg, J.S., Abudayyeh, O.O., Kellner, M.J., Joung, J., Collins, J.J., and Zhang, F. (2018). Multiplexed and portable nucleic acid detection platform with Cas13, Cas12a, and Csm6. *Science* 360, 439–444.
24. Li, B., Zeng, C., Li, W., Zhang, X., Luo, X., Zhao, W., Zhang, C., and Dong, Y. (2018). Synthetic oligonucleotides inhibit CRISPR-Cpf1-mediated genome editing. *Cell Rep.* 25, 3262–3272.e3.
25. Gao, L., Cox, D.B.T., Yan, W.X., Manteiga, J.C., Schneider, M.W., Yamano, T., Nishimasu, H., Nureki, O., Crosetto, N., and Zhang, F. (2017). Engineered Cpf1 variants with altered PAM specificities. *Nat. Biotechnol.* 35, 789–792.
26. Tu, M., Lin, L., Cheng, Y., He, X., Sun, H., Xie, H., Fu, J., Liu, C., Li, J., Chen, D., et al. (2017). A 'new lease of life': FnCpf1 possesses DNA cleavage activity for genome editing in human cells. *Nucleic Acids Res.* 45, 11295–11304.
27. Świat, M.A., Dashko, S., den Ridder, M., Wijsman, M., van der Oost, J., Daran, J.-M., and Daran-Lapujade, P. (2017). FnCpf1: a novel and efficient genome editing tool for *Saccharomyces cerevisiae*. *Nucleic Acids Res.* 45, 12585–12598.
28. Apweiler, R., Bairoch, A., Wu, C.H., Barker, W.C., Boeckmann, B., Ferro, S., Gasteiger, E., Huang, H., Lopez, R., Magrane, M., et al. (2004). UniProt: the Universal Protein knowledgebase. *Nucleic Acids Res.* 32, D115–D119.
29. Brett, M., Doppalapudi, A., Respicio-Kingry, L.B., Myers, D., Husband, B., Pollard, K., Mead, P., Petersen, J.M., and Whitener, C.J. (2012). *Francisella novicida* bacteremia after a near-drowning accident. *J. Clin. Microbiol.* 50, 2826–2829.
30. Connelly, J.C., and Leach, D.R.F. (1996). The sbcC and sbcD genes of *Escherichia coli* encode a nuclease involved in palindrome inviability and genetic recombination. *Genes Cells* 1, 285–291.
31. Connelly, J.C., Kirkham, L.A., and Leach, D.R.F. (1998). The SbcCD nuclease of *Escherichia coli* is a structural maintenance of chromosomes (SMC) family protein that cleaves hairpin DNA. *Proc. Natl. Acad. Sci. USA* 95, 7969–7974.
32. Connelly, J.C., de Leau, E.S., and Leach, D.R.F. (1999). DNA cleavage and degradation by the SbcCD protein complex from *Escherichia coli*. *Nucleic Acids Res.* 27, 1039–1046.
33. Lim, C.T., Lai, P.J., Leach, D.R., Maki, H., and Furukohri, A. (2015). A novel mode of nuclease action is revealed by the bacterial Mre11/Rad50 complex. *Nucleic Acids Res.* 43, 9804–9816.